[2] Dryden, H. L., *Advances in Applied Mechanics*, Vol. 1, Academic Press, New York, 1948, pp. 1–40.

[3] Bradshaw, P., Ferriss, D. H., and Atwell, N. P., "Calculation of Boundary Layer Development Using the Turbulent Energy Equation," *Journal of Fluid Mechanics*, Vol. 28, Pt. 3, 1967, pp. 593–616.

[4] Lee, S. C., "A Study of the Two-Dimensional Free Turbulent Mixing between Converging Streams with Initial Boundary Layers," Ph.D. dissertation, 1966, Univ. of Washington, Seattle, Wash.

[5] Zawacki, T. S. and Weinstein, H., "Experimental Investigation of Turbulence in the Mixing Region between Coaxial Streams," CR-959, Feb. 1968, NASA.

[6] Heskestad, G., "Hot-Wire Measurements in a Plane Turbulent Jet," *Journal of Applied Mechanics*, Vol. 32, 1965, pp. 721–724.

[7] Heskestad, G., "Hot-Wire Measurements in a Radial Turbulent Jet," *Journal of Applied Mechanics*, Vol. 33, 1966, pp. 417–424.

[8] Spalding, D. B. and Patankar, S. V., *Heat and Mass Transfer in Turbulent Boundary Layers*, Chemical Rubber Co. Press, Cleveland, 1968.

[9] Patankar, S. V. and Spalding, D. B., "A Finite-Difference Procedure for Solving the Equations of the Two-Dimensional Boundary Layer," *International Journal of Heat and Mass Transfer*, Vol. 10, 1967, pp. 1389–1411.

[10] Townsend, A. A., *The Structure of Turbulent Shear Flow*, Cambridge University Press, Cambridge, 1956.

[11] Hinze, J. O., *Turbulence*, McGraw-Hill, New York, 1959.

[12] Sami, S., "Velocity and Pressure Fields of a Diffusing Jet," Ph.D. dissertation, 1966, Univ. of Iowa, Iowa City.

[13] Peters, C. E., Chriss, D. E., and Paulk, R. A., "Turbulent Transport Properties in Subsonic Coaxial Free Mixing Systems," AIAA Paper 69–681, San Francisco, Calif., 1969.

JUNE 1970 AIAA JOURNAL VOL. 8, NO. 6

Transpiration and Film Cooling Effects for a Slender Cone in Hypersonic Flow

C. R. WIMBERLY* AND F. K. MCGINNIS III†
LTV Aerospace Corporation, Dallas, Texas

AND

J. J. BERTIN‡
University of Texas, Austin, Texas

Tests were conducted in the LTV Aerospace Corporation (Vought Aeronautics Division) Hypervelocity Wind Tunnel to determine transpiration and film cooling effects on the aerodynamic characteristics of a slender cone in hypersonic flow. Film cooling of the model was obtained by injecting methane out of and near the slightly truncated nose. Transpiration cooling was provided by injecting ethylene through the remaining surface of the model. The resulting effects on heat transfer, skin friction, and pressure distribtions, and force and moment data are analyzed and discussed. The flow conditions were limited to nominal Mach numbers of 12 and 17, and respective Reynolds numbers per ft of 6×10^6 and 10^6. It was found that the heat transfer, skin friction, axial force coefficient, and normal force coefficient slope decreased with increased mass injection for both film and transpiration cooling. The effectiveness of film cooling, however, decreased with distance from the injection region, and diminished with increased angle of attack. It was observed from test results and photographs that boundary-layer transition was induced by light mass injection at the higher Reynolds number.

Nomenclature

A = area
C = Chapman-Rubesin coefficient, $\rho\mu/(\rho\mu)_{ref}$
C_A = axial force coefficient with base pressure assumed to be zero
$C_{A'}$ = axial force coefficient with base pressure equal to the free-stream value
C_D = drag coefficient
C_f = skin-friction coefficient
C_i = injection parameter, $\dot{m}/\rho_\infty V_\infty A_b$
C_M = moment coefficient
C_N = normal force coefficient
C_P = pressure coefficient
c_p = specific heat at constant pressure
d = diameter
k = thermal conductivity
L = model length
$\dot{m}$ = injected mass flow rate (total)
M = Mach number
P = static pressure
Pr = Prandtl number, $c_p\mu/k$
$\dot{q}$ = heat-transfer rate
r = radius
Re_x = Reynolds number, $\rho_e V_e x/\mu_e$
St = Stanton number, $\dot{q}/\rho c_p V(T_r - T_w)$
t = time
T = temperature
V = inviscid stream velocity
W = vehicle weight
x = station on cone (distance from apex)
x' = axial distance from aftmost point of mass injection
α = angle of attack
β = ballistic coefficient $W/C_D A_b$
γ = entry angle
θ_c = cone half angle
μ = viscosity
ρ = density

Received June 23, 1969; revision received November 17, 1969.

* Senior Specialist, Vought Aeronautics Division. Member AIAA.

† Engineering Specialist, Missiles and Space Division. Member AIAA.

‡ Assistant Professor, Aerospace Engineering Department. Member AIAA.

Subscripts

c = cone
b = base
E = entry conditions
inj = injected
n = nose
o = no-blowing value
r = recovery
ref = reference condition
T = total
w = wall
x = location defined by x
∞ = freestream

Introduction

MATERIALS such as graphite and the composite ablators have recently constituted the typical forms of thermal protection for the nosetip of re-entry vehicles. The simplicity, reliability, and thermal efficiency of such systems make them the obvious choice for blunted re-entry vehicles and moderate ballistic trajectories. However, for high ballistic coefficients and shallow entry angle trajectories currently under consideration a relatively sharp nosetip becomes exposed to an environment of such severity as to render these materials useless. In particular, the high stagnation temperatures and pressures associated with such trajectories result in severe thermal and mechanical erosion of these materials. Consequent nose blunting decreases the effective ballistic coefficient of the vehicle and, hence, degrades vehicle performance. An acknowledged solution to this problem involves the use of an active cooling system. Thus, the actively cooled nosetip (the subject of considerable work during the last decade) is once again being considered as a means of protecting the forebody of a re-entry vehicle.

The class of re-entry vehicles under consideration here possesses a transpiration cooled nosetip and a conventionally (charring ablator) protected afterbody where tip mass injection and afterbody outgassing occur simultaneously. To simulate the effects, a conical re-entry configuration with a porous skin and a slightly truncated tip was selected to be tested at the expected entry conditions. Although the individual problems, i.e., transpiration cooling in stagnation regions and distributed mass injection on an axisymmetric body, have been thoroughly investigated,[12-22] the data have been quite scattered and the combined problems involving the mixing of three different fluids (freestream gas, tip coolant, and ablation products) have not been studied. In order to gain some insight into the multiple interactions which occur in this situation and to evaluate techniques for the prediction of aerodynamic characteristics and heat transfer under these conditions, an exploratory experimental investigation was undertaken, jointly sponsored by the Missiles and Space Division in Texas (MST/T) and the Vought Aeronautics Division (VAD) of the LTV Aerospace Corporation. The test facility used in the program was the VAD Hypervelocity Wind Tunnel.

Since it was desired to simulate the actual vehicle design and flight conditions as closely as possible, considerable effort was put forth in the selection of flow conditions and injected substances. Two flow conditions were selected to simulate the early and peak heating portions of a ballistic entry trajectory with $V_E = 26000$ fps, $\gamma_E = -3°$, and $\beta = 15000$ psf. During the early, high-altitude part of the trajectory the flow is laminar and the tip mass injection is much larger than the outgassing. Under these conditions the effects of mass injection upon vehicle aerodynamic characteristics are of primary interest. During the maximum heating portion of the trajectory, the flow is turbulent and the outgassing dominant. The two flow conditions at these points in flight correspond closely to Mach and Reynolds number combinations of 1) $M_\infty = 17$, $Re/\text{ft} = 1.0 \times 10^6$ and 2) $M_\infty = 12$, $Re/\text{ft} = 6.0 \times 10^6$, respectively, and were the selected nominal conditions for the test program.

The injected gases were chosen to simulate the injection of steam from the tip and carbon phenolic ablation products from the afterbody. Water has been shown to be the optimum transpiration coolant from the over-all system weight/performance standpoint. However, the low-heating rates encountered in the HVWT precluded the use of liquid coolants. Thus, simulation of freestream-to-injected molecular weight ratio was the primary consideration, with specific heat ratio simulation also desired. Considering these objectives and limitations, methane (CH_4) and ethylene (C_2H_4) were chosen to simulate the steam and the ablation products, respectively.

Test Facility

The test facility used in the program was the VAD Hypervelocity Wind Tunnel which is an arc-heated, hotshot type tunnel with a variable volume arc chamber that results in long run times (300 msec maximum) and constant flow conditions during a run. The tunnel has a 7.5° total-included-angle conical nozzle which terminates in a 13-in. diam test section. Flow conditions in the test section are obtained during each run with pressure measurements and a special total-temperature probe.

To operate the tunnel a gas is quickly heated in the arc chamber volume, followed by a reduction in the volume to maintain a high, postarc pressure level until all of the gas is expended through the nozzle. This reduction in volume is accomplished with a piston forming the rear wall of the arc chamber. The piston is driven by high-pressure nitrogen and its release and speed are controlled with hydraulic back pressure. The valve mechanism used to open the arc-chamber to the nozzle provides little or no fragmentation in the flow that is normally associated with the conventional diaphragm methods. As a result, flow contamination and particle damage to the model were negligible.

The arc-chamber pressure was measured with a strain-gage type transducer while test section pressures were measured with either this type instrument or variable reluctance transducers, depending upon the anticipated magnitude of the particular pressure. Test-section after-shock total temperature was measured with a probe specifically designed for this purpose. Aerodynamic forces were measured with the VSB-1 semiconductor balance which has four separate gas supply channels routed through it. The balance, which was designed and fabricated at VAD, is insensitive to pressure in the gas supply channels. A more detailed description of the facility is contained in Ref. 1.

Model and Test Procedure

The model tested during this program was a 7.25° half-angle cone slightly truncated with a nose-to-base radius ratio of 0.017. The surface of the model was fabricated from a sintered nickel porous skin through which gases were injected into the flowfield. Internally the model had four compartments for the control of the mass-injection distribution. A drawing of the model is shown in Fig. 1. Compartment 1 consisted of an 0.034-in. diam orifice at the nose (hand-finished OD $\approx$ 0.038-in.). Compartment 2 was a small circumferential volume in the nose region while Compartments 3 and 4 comprised the rearmost 91.9% of the actual model length and were separated by a midline divider. The forward $\frac{1}{8}$-in. of Compartment 2 was a "dead" area which resulted from the joining of the Compartment 1 tube with the model skin. Methane was supplied to Compartments 1 and 2 while ethylene was the injectant for Compartments 3 and 4.

The porous skin was fabricated from 0.006-in. thick sheet stock (Union Carbide NR-30) which was formed into a cone and electron beam welded along a ray. The porosity of the

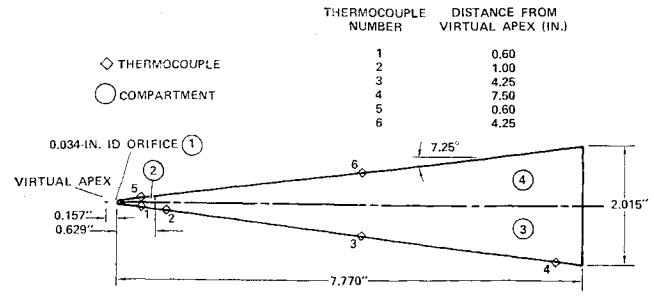

Fig. 1 Test model.

skin was found to be highly uniform through measurements of hot wire velocity distributions and by comparing increased pressure measurements (of a small low-pressure reservoir) caused by several sample plugs of the skin material. The inner shell was machined from magnesium and glands were provided in each bulkhead and divider. A silicone rubber material was formed into these glands to afford sealing surfaces with the porous skin and thus prevent leakage between adjacent compartments.

The system which was used to supply gas at the required pressure to each compartment consisted of four separate supply lines each equipped with a regulator, pressure gage, and solenoid valve. A small diameter restriction, located in each of the supply channels of the balance, was utilized as a sonic orifice in a calibration procedure in which mass flow rate was determined as a function of supply pressure and temperature. Using this calibration technique for each of the supply systems, it was possible to obtain the supply pressure required for a desired mass flow rate for each compartment. Injection rates per compartment were shown to be higher near the front of the model (when compared with the aft injection rates) since the supply system was initiated there, decreasing thereafter asymptotically to a near uniform distribution at the aft end of the compartment. The injection parameter, C_i, was calculated for each compartment using the injected mass flow indicated by the supply gage settings and freestream mass flux during the particular run.

Heat-transfer data were obtained from chromel/constantan thermocouples which were resistence welded to the porous model skin. After the test program a master calorimeter was fabricated for calibration purposes and attached to the model aligned with the windward ray. The master calorimeter was carefully made from copper sheet (0.0046-in. thick) and with these characteristics well defined, the calorimeter equation was used for the calculation of heat-transfer rate when a radiant heat source was applied. Heating rates at each sensing location were computed from the measured temperature histories, dT/dt, which were established by determining the "best" straight line through each of the temperature traces on the oscillograph records.

The tunnel flow parameters and the force data were reduced by an IBM 7090 digital computer which printed out listings of the pertinent flow conditions and the force coefficients for every millisecond of run time. Tunnel flow conditions were calculated using an input of arc chamber pressure and test section after-shock values of total pressure and total temperature. The force coefficients were computed from the balance gage loads and were corrected for the load interactions defined by calibration.

A summary of the test conditions and data for the program is shown in Table 1. Additional information on the test procedure and program can be obtained from Ref. 2.

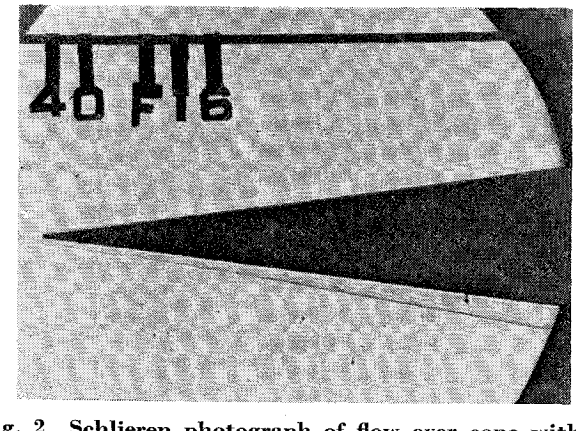

Fig. 2 Schlieren photograph of flow over cone without mass injection, $M_\infty = 12.2$ Re_∞/ft. $= 6.89 \times 10^6$/ft, $\alpha = 0$.

Discussion of Results

The inviscid flowfield was defined using schlieren photographs, heat-transfer rates, and force-and-moment measurements in the pitch plane. Schlieren photographs of the flowfield for the high Reynolds number flow past the cone at zero incidence with and without mass injection are presented in Figs. 2 and 3, respectively. For the zero-injection flowfield, the shock wave geometry, as shown in Fig. 2, compares favorably with the 9° half-angle conical shock predicted from sharp cone theory.[3] Some weak disturbances in the zero-injection flowfield are indicated by the Mach waves in Fig. 2, possibly caused by small surface irregularities.

Since the model was not instrumented for pressure measurements, a correlation of data from similar, slightly blunted cones was assumed to represent the pressure distribution.[4] This correlation also compares favorably with the recomputed pressure coefficients measured by Lewis[5] using a similar model at flow conditions not too different from those of the present program. A hot shot type hypervelocity wind tunnel was also used in obtaining these pressure data. According to Griffith and Lewis,[5] the relatively small bluntness affects the pressure over the entire model surface area with the asymptotic value greater than that predicted using sharp-cone theory. An overexpansion occurs near the nose, followed by a recompression and a monotonic approach to the asymptotic value. Using this pressure distribution one computes a Mach angle of 6.4°, which corresponds closely to the 6° wave appearing in the schlieren photograph of Fig. 2.

Although some differences in shock shape with and without blowing are shown in Figs. 2 and 3, the pressure distribution was assumed to be only slightly affected by mass injection for the conditions of the current program (Table 1). This assumption was based on an iterative correlation of the test data where a slight reduction in aft pressure was required to provide agreement with force measurements for tests with mass injection. The assumption is also supported by Hillsamer and Mallard,[6] who found that gases injected near the apex of both sharp and blunted conical models, resulted in either no change or a decrease in the surface pressure and by Studerus,[7] who showed only minor changes in pressure with mass injection normal to the surface and $C_i < 0.04$. Consequently, the pressure distribution without mass injection was also assumed to represent the pressure field for the light mass injection rates used in the program.

The heat-transfer measurements in terms of the Stanton number are presented for the no-injection runs in Fig. 4 as a function of the local Reynolds number. The data are compared with the sharp cone theoretical relation[8]

$$St = [0.575/(Pr)^{0.667}]\,(C/Re_x)^{1/2}$$

The local flow properties necessary to compute the Stanton number and the Reynolds number were calculated using the assumed pressure distribution. The equation suggested by Probstein and Elliott[9] was used to estimate the transverse curvature effect. Changes induced by interactions between the viscous boundary layer and the inviscid shock layer were

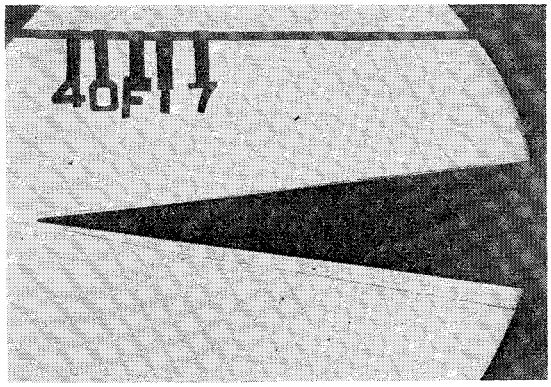

Fig. 3 Schlieren photograph of flow over cone with mass injection, $M_\infty = 12.1$, $Re_\infty/\text{ft} = 6.36 \times 10^6/\text{ft}$, $\alpha = 0$.

estimated using the relation suggested by Probstein.[10] For the Mach 17 flow these two corrections indicate a 25% increase in heat transfer at the foremost thermocouple and a 7% increase at the most downstream thermocouple. Because of the reduced boundary-layer thickness for the Mach 12 flow, the combined effect of viscous interaction and transverse curvature does not exceed 5%. The agreement between the predicted and measured heat-transfer data is satisfactory considering the uncertainty in the definition of the inviscid flowfield. The relatively flat heat-transfer distributions (which differ significantly from the $x^{-1/2}$ predicted by sharp-cone theory) are attributed to tip-blunting, since heat-transfer rates measured on a sharp cone from a previous test in this facility correlate very well with theory.[11]

Heat-transfer distributions for the Mach 17 runs with tip injection (i.e., film cooling) displayed consistent trends. At the lower injection rates, the magnitude of the heat transfer near the tip was significantly reduced, but downstream distributions rapidly approached the laminar, no-injection values. As the injection rate was increased, uniform heating was approached, with all heat flux levels far below the laminar, no-injection values. Thus, tip mass injection significantly affected both the local and the downstream heat-transfer rates. Libby and Cresci[12] investigated the downstream influence of stagnation-region injection. However, their work was confined to a relatively blunt body and utilized low injection rates. Brunner[13] discussed data taken in an axisymmetric flow situation, but again the model tested was relatively blunt and, in addition, model ablation effects were present. Thus, the results presented herein appear to be unique. Consequently, the recent work of Carlson and Talmor[14] was used to establish correlation parameters. Although particularly concerned with an accelerating two-dimensional, compressible turbulent flow with film cooling, Carlson and Talmor developed a mixing model which correlates the available data satisfactorily. With this background, the following parameter

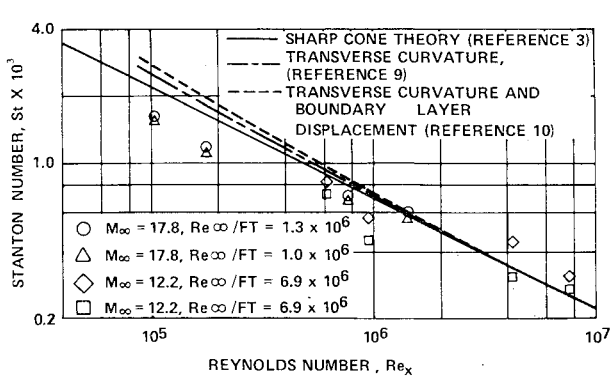

Fig. 4 Stanton number variation without mass injection, $\alpha = 0$.

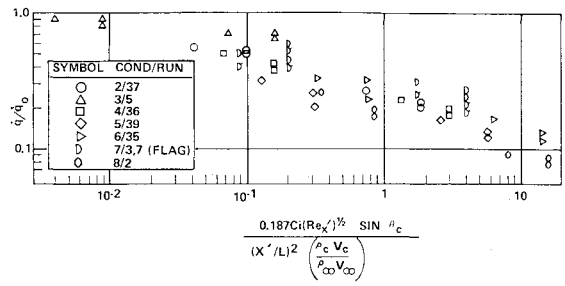

Fig. 5 Reduced heating rate due to film cooling, $M_\infty = 17.8$, $Re_\infty/\text{ft} = 1.3 \times 10^6/\text{ft}$, $\alpha = 0$.

was used to represent the dilution of the effect of tip mass injection with distance from the injection location in an axisymmetric laminar flow:

$$C_i(Re_{x'})^{1/2}\sin\theta_c/[(x')^2/L]\ (\rho_c V_c/\rho_\infty V_\infty),\ (0.0 < x'/L \leq 1)$$

The dependent variable was taken to be reduced heat flux, $\dot{q}/\dot{q}_0$, which is a measure of the film cooling effectiveness. Data presented in terms of these parameters are shown in Fig. 5.

Data taken for tip mass injection with the model at a slight angle of attack were few, but some qualitative observations can be made. Angle of attack was found to greatly reduce film cooling effectiveness with the most significant reduction occurring during the initial 2° angle-of-attack increment. Apparently, only a minimal crossflow was necessary to cause a major deterioration of the film cooling effectiveness for the model configuration and injection rates of the study.

At the Mach 12 flow condition, afterbody mass injection dominated from a total mass injection standpoint, although tip mass injection was still present as indicated in Table 1. Because the high Reynolds number flow is susceptible to mass-injection-induced boundary-layer transition, the trends indicated by the heat-transfer data were more complex, but nonetheless clear. The minimum injection rate investigated resulted in a reduction in the heat flux at all thermocouples. Increases in injection rate resulted in a further reduction in heat transfer near the tip, accompanied by increased heat transfer to the afterbody. The increase is attributed, at least in part, to boundary-layer transition, and the indication that the transition point moved forward as injection rate increased was verified by the schlieren photographs. It should be noted that the heat-transfer rates at the aft end of the model exceeded the no-injection (laminar flow) values only at the highest injection rates. Thus, the turbulent portion of the boundary layer was significantly affected by the afterbody mass injection, as one would anticipate. Finally, the data indicate a strong effect of tip mass injection at constant afterbody mass injection. It was apparent that small

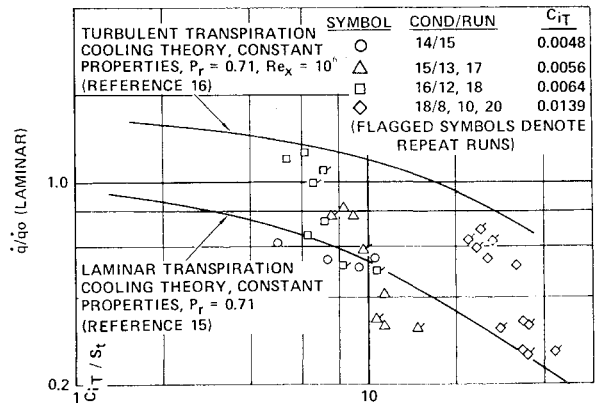

Fig. 6 Reduced heating rate due to transpiration cooling, $M_\infty = 12.2$, $Re_\infty/\text{ft} = 6.5 \times 10^6/\text{ft}$, $\alpha = 0$.

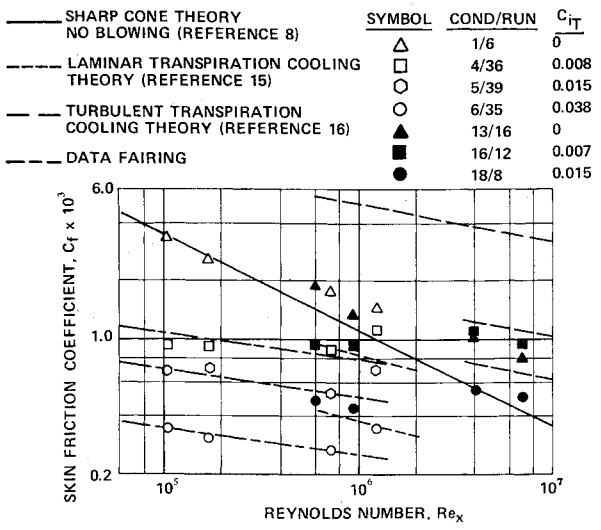

Fig. 7 Skin-friction coefficient, $\alpha = 0$.

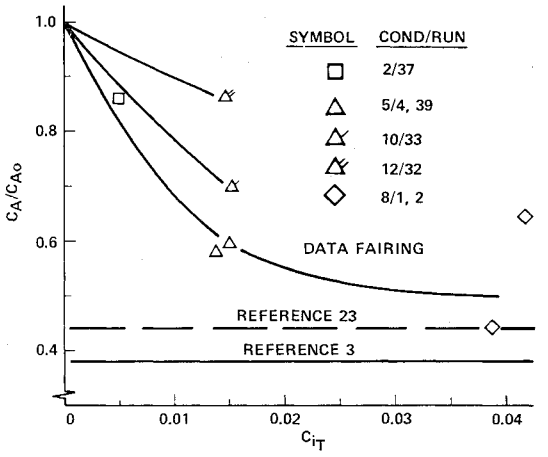

Fig. 8 Effects of film cooling and angle of attack on axial force coefficient.

changes in tip mass injection greatly affected the transition point, other parameters remaining constant.

Transpiration cooling has been studied for many years, and it is thus logical that the results of the present work be compared with existing theories and experimental results. Distributed mass injection has been treated analytically by Rubesin[15] for laminar flow and Rubesin and Pappas[16] for turbulent flow and summarized by Kelley et al.[17] Correlation techniques applicable to laminar transpiration cooling problems involving air and nonair freestreams are given in the very recent work of Simon et al.[18] Experimental investigations particularly concerned with slender bodies of revolution are presented in Refs. 19, 20, and 21. The results are generally presented in terms of a reduced heat flux or Stanton number as a function of a mass injection parameter. The Mach 12, zero angle-of-attack data of the present work are presented in this form in Fig. 6. The parameter C_{iT}/St is analogous to the parameter B of Refs. 15 and 16, the difference arising from the fact that the present work involved nonuniform mass injection. The theoretical laminar and turbulent flow results of Refs. 15 and 16 are also shown in Fig. 6. Because the blowing distribution was a step function using dissimilar gases and because the influence of injectants on the inviscid flow properties has been neglected, the agreement between the data and theory is considered satisfactory. Some of the data agree rather well with the laminar theory. Further inspection reveals that the data points in poor agreement with the laminar theory correspond to aft locations,

Table 1 Test data summary

TEST COND. NO.	RUN NO.	M	R/ℓ PER FT.	α DEG.	C_{i_1}	C_{i_2}	C_{i_3}	C_{i_4}	HEAT TRANSFER RATES BTU/FT.² SEC. T/C 1	T/C 2	T/C 4	T/C 5	T/C 6	T/C 7	FORCE DATA C_N	C_m	C_m/C_N	C_A	C_A'	C_B
1	6	17.81	1.28	0	0	0	0	0	5.313	4.263	3.167	2.658	5.417	2.968	.0017	-.0012	-	.07381	.06930	.00269
1	38	17.80	1.02	↓	↓	↓			5.074	4.143	3.085	2.540	5.161	2.763	.00154	-.00105	-	.07345	.06894	.00687
2	37	18.07	0.99		.00012	.00482			1.164	1.136	1.580	1.436	1.101	1.505	.00148	-.00081	-	.06343	.05906	.00703
3	5	18.62	1.12		.00043	0			3.888	3.448	2.818	2.308	4.235	2.646	.0009	-.0007	-	.08189	.07777	.00316
4	36	17.69	0.99		.00038	.00761			1.013	0.961	1.178	1.314	1.008	1.201	.00264	-.00165	-	.05232	.04775	.00719
5	4	17.83	1.34		.00034	.01352			0.390	0.364	0.436	0.526	0.374	0.406	.0016	-.0009	-	.04284	.03835	.00275
5	39	17.68	1.07		.00037	.01465			0.676	0.674	0.661	0.860	0.675	0.739	.00344	-.00221	-	.04384	.03927	.00731
6	35	17.78	1.04		.00038	.03765			0.732	0.729	0.741	0.860	0.717	0.900	.01560	-.00868	-	.03985	.03533	.00559
7	3	17.97	1.29		.00104	0			1.442	1.500	1.592	1.319	1.535	1.553	-.0011	.0002	-	.07742	.07299	.00175
7	7	18.01	1.31		.00103	↓			1.779	1.893	2.003	1.667	2.062	1.879	.0001	-.0003	-	.07019	.06579	.00254
8	1	17.11	1.37		.00094	.03780			0.251	0.215	0.281	0.316	0.232	0.302	.0034	-.0019	-	.03287	.02795	.00021
8	2	18.07	1.46	↓	.00102	.04073			0.331	0.299	0.392	0.426	0.327	0.357	.0036	-.0020	-	.04774	.04336	.00981
9	34	17.91	1.03	2	0	0			5.057	4.197	2.952	2.323	4.242	1.964	.05869	-.03839	-.654	.07180	.06734	.00995
10	33	17.67	1.05	↓	.00037	.01477			1.796	1.516	2.105	2.063	1.668	1.326	.05559	-.04183	-.752	.05012	.04554	.01062
11	31	17.44	1.07	4	0	0			5.393	5.612	3.711	3.013	4.126	2.155	.10405	-.06728	-.647	.07533	.07063	.00845
12	32	17.41	1.03	↓	.00035	.01411			2.168	2.061	3.557	2.649	1.761	1.696	.11210	-.07934	-.708	.06454	.05983	.00696
13	14	12.11	6.94	0	0	0			17.856	15.546	13.253	10.141	22.342	15.466	.00100	-.00077	-	.03996	.03021	.03732
13	16	12.20	6.89	↓	↓	↓	↓	↓	17.645	12.268	9.230	8.665	17.366	10.629	.00130	-.00101	-	.04557	.03595	.04169
14	15	12.17	6.69		.000040	↓	.00240	.00240	10.926	7.470	5.828	5.143	10.279	4.757	.00059	-.00049	-	.04123	.03158	.03911
15	13	12.12	6.16		.000042	.00084	.00251	.00251	5.640	5.652	8.402	7.661	4.871	6.689	.00044	-.00064	-	.04061	.03088	.03710
15	17	12.10	6.36		.000041	.00082	.00247	.00247	5.934	4.322	6.525	7.013	5.499	5.983	-.00007	-.00030	-	.03865	.02887	.03283
16	12	11.87	6.18		.000042	.00166	.00249	.00249	11.158	10.159	13.510	11.881	10.394	12.120	.00074	-.00050	-	.05721	.04706	.03986
16	18	12.12	6.55		.000041	.00162	.00243	.00243	9.000	6.755	11.009	10.173	6.957	8.446	.00092	-.00059	-	.04478	.03505	.03549
17A	11	12.52	6.87		.000042	.00425	0	0	7.373	6.260	9.138	8.217	6.430	8.632	.00290	-.00178	-	.05635	.04724	.04167
17A	19	11.99	5.74		.000042	.00420	↓	↓	9.898	10.259	14.316	14.704	13.546	15.520	.00067	-.00067	-	.04682	.03687	.03697
18	8	12.35	7.70		.000121	.00484	.00454	.00454	4.684	4.585	6.096	4.824	4.271	6.343	.00244	-.00174	-	.05115	.04175	.03410
18	10	12.43	7.26		.000122	.00488	.00457	.00457	4.460	3.545	6.579	5.815	3.930	5.986	.00286	-.00184	-	.04879	.03954	.03510
18	20	12.21	6.54	↓	.000127	.00506	.00475	.00475	5.545	4.448	7.022	6.398	6.032	7.061	.00234	-.00129	-	.05613	.04654	.04297
19	21	12.17	6.13	2	0	0	0	0	21.348	19.083	14.462	12.521	16.708	10.917	.05136	-.03369	-.656	.04476	.03511	.04322
20	22	12.34	6.73		.000043	.00172	.00258	.00258	8.705	8.515	14.122	10.475	7.754	8.765	.06166	-.04069	-.660	.03170	.02231	.02355
20	23	12.30	7.02		.000041	.00164	.00245	.00245	6.735	7.331	10.403	9.773	7.334	8.520	.05835	-.03923	-.672	.04444	.03498	.02565
20	24	12.01	5.80		.000042	.00169	.00254	.00254	8.197	7.551	11.568	10.394	7.199	8.475	.05907	-.03955	-.670	.05075	.04159	.04415
21	25	12.26	6.80	↓	.000041	.00164	.00400	.00133	6.986	6.376	11.163	9.867	6.378	7.611	.05844	-.03880	-.664	.05194	.04242	.03764
22	26	12.34	6.88	4	0	0	0	0	27.375	21.984	16.928	15.450	15.128	11.775	.10397	-.06731	-.647	.03891	.02952	.02552
22	28	12.29	7.15		↓	↓	↓	↓	27.558	22.861	15.536	12.853	13.483	9.386	.10951	-.07038	-.644	.04944	.03995	.02569
23	40	11.86	7.28		.000039	.00154	.00231	.00231	13.000	15.891	17.789	14.040	11.617	10.006	.09300	-.06093	-.655	.05611	.04594	.01162
24	41	11.76	6.75	↓	.000036	.00144	.00513	0	14.736	16.967	18.790	15.968	15.241	10.538	.10805	-.06967	-.645	.05793	.04760	.04669
											FASTAX SHOTS									
20	42	12.28	6.06	2	.000045	.00178	.00268	.00268	10.036	11.966	13.849	11.206	10.913	10.508	.05955	-.03917	-.658	.05938	.04991	.02814
20	43	12.26	6.07	↓	.000044	.00177	.00265	.00265	11.861	10.208	12.896	11.535	11.138	9.236	.06006	-.03950	-.658	.06352	.05401	.02716
24	44	12.10	6.44	4	.000042	.00166	.00593	0	14.400	15.132	15.335	14.979	14.485	11.103	.11707	-.07585	-.648	.06567	.05590	.05974
											OTHER SHOTS									
-	45	17.02	1.16	0					4.586	3.581	2.790	2.290	4.835	2.512	-.00079	.00044	-	.06317	.05824	.00275
-	46	17.70	1.04	↓	0	.000136	.00996	.01001	-	1.783*	1.415	1.082	3.327	1.305	.00201	-.00175	-	.05227	.04771	.00644

*T/C 3

where injection-induced turbulence was observed in the flow-visualization photographs. In light of this information, the data for the forward thermocouples, which apparently were exposed to a purely laminar flow, were compared with the results of Ref. 21, which were obtained at a Mach number of 5 and freestream unit Reynolds number of 1.2 (10^6)/ft. The agreement was quite satisfactory.

Force and moment data, which were taken concurrently with the heat-transfer measurements, are presented in Table 1 as force coefficients (assuming the base pressure to be zero and freestream) and moment coefficients. An effort was made to separate the total measurements into pressure and skin-friction contributions, although neither was measured. The assumed pressure field has been discussed. The skin-friction contribution was calculated using Reynolds analogy for hypersonic flow with the Stanton numbers determined using the thermocouple measurements. Danberg et al.[22] found that the relation between the skin-friction coefficient and the Stanton number varied with the mass-injection rate. However, for the mass-injection rates of the current program, the variation is small and the constant ratio of Reynolds analogy was assumed valid. Values of the resulting skin-friction coefficients for the cone at $\alpha = 0°$ are shown in Fig. 7. The no-injection coefficients are compared with the sharp-cone relation.[8] As shown, the skin-friction coefficients calculated using the heat-transfer data for the no-injection cases correlate reasonably well with theory, with slightly closer agreement at Mach 17. At these conditions (low Reynolds number), the skin-friction coefficient decreases continuously with increased mass injection, as illustrated by data fairings (Fig. 7), where the gas (methane) is injected into the flow only through the two foremost compartments, simulating film cooling. For the high Reynolds number flow ($M_\infty = 12$), gases (methane and ethylene) are injected from all four compartments, simulating both film and transpiration cooling, for the model. As noted for these runs, the skin-friction coefficients based on the heat-transfer data indicate that mass injection has promoted boundary-layer transition. The skin-friction coefficients for the aft portion of the cone correlate reasonably well with the transpiration cooling for a turbulent boundary layer. Comparisons of integrated values of the pressure and skin-friction contributions and the measured force data are shown in Table 2 and indicate reasonable agreement considering the uncertainties in obtaining distributed properties.

Only limited data were obtained at angle of attack; however, some interesting results are suggested by the axial force coefficient data shown in Fig. 8. A typical and rather large reduction occurs at $\alpha = 0$ with increasing mass injection at the tip, approaching the viscous interaction theory of Whitfield and Griffith[23] and the inviscid predicted values of Sims.[3] As indicated by Studerus[7] et al, this is due primarily to a reduction in skin friction since the initial effect of mass injection on the pressure is slight. The decreased effectiveness of mass injection on C_A/C_{A0} at $\alpha = 2$ and 4° is attributed to a thinner boundary layer and greater shear stresses on the

Table 2 C_A data comparison with mass injection, $\alpha = 0$

$M_\infty = 12$			$M_\infty = 17$		
C_{iT}	From local data	Force tests	C_{iT}	From local data	Force tests
0	0.056	0.040 0.046	0	0.061	0.073 0.063
0.0064	0.054	0.045 0.057	0.0076	0.052	0.052
0.0139	0.052	0.049 0.051	0.0146	0.049	0.044
			0.0376	0.047	0.040

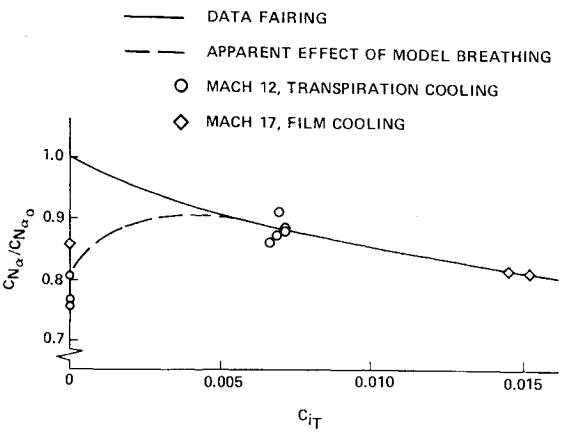

Fig. 9 Effects of film and transpiration cooling on normal force coefficient slope.

windward side (but still less than values without blowing) caused primarily by higher pressure there and cross flow.

The effect of mass injection on the normal force coefficient slope, normalized to the nonporous, no-injection blunt-cone data correlation of Whitfield and Wolny,[24] is shown in Fig. 9 and agrees with the results of Eckstrom,[25] indicating that film and transpiration cooling initially reduce $C_{N\alpha}$. The porosity of the model apparently caused some noticeable configuration breathing (defined here as an uncontrolled and probably nonuniform mass flow through the surface) for zero mass injection, resulting in a significantly lower value of $C_{N\alpha}$, as shown. It is likely that breathing did not occur with mass injection. The reduction of $C_{N\alpha}$ with mass injection can be explained in part by using arguments of Chrusciel and Chang[26] where cross flow at angle of attack, highly induced by mass injection, causes pockets of high-pressure regions on the leeward side, thus contributing to the reduction. Another consideration is the obvious change in shock shape with mass injection and cone incidence which would alter the pressure differential and reduce $C_{N\alpha}$.

Conclusions

The nature of the test program for film and transpiration cooling effects at hypersonic speeds was exploratory, resulting in the investigation of many effects. This caused a limited amount of data for each effect; however, analyses of the data for the distributed heat transfer, forces, and moments and the schlieren photographs yielded interesting conclusions as follows.

1) Film cooling resulted in a significant decrease in heat transfer over the surface and in values of the axial force coefficient. The effectiveness of film cooling on heat transfer, however, decreased with distance from the cooling region and with angle of attack. Its effectiveness on force data also decreased with angle of attack. The injection of the coolant in the tip region did not induce transition for this lower Reynolds number flow.

2) Gas injection from all compartments (simulating local ablation or transpiration cooling as well as film cooling) led to a more complex flowfield. Premature boundary-layer transition did occur as a result of the higher Reynolds numbers and distributed mass injection, resulting in higher local heating rates above the no-injection values.

3) A reduction in the normal force coefficient slope was observed with increased mass-injection rate for both film and transpiration cooling.

4) Apparently, breathing through the model skin reduced the values of the normal force coefficient slope for the no-injection runs, although no identifiable effect could be seen in the heat-transfer data. The effect was not present for the tests with mass injection.

References

[1] J. L. Lindsey, "Hypervelocity Wind Tunnel Handbook," Publication 2-59740/4R-2150, Sept. 1964, LTV Aerospace Corp., Dallas, Texas.

[2] T. C. Pope, C. J. Stalmach, Jr., and J. L. Lindesy, "Aerothermodynamic Measurements on a Cone Simulating a Transpiration Cooled Tip and an Ablating Heatshield at Mach 17 and 12," Rept. 2-59740/8R-2511, Sept. 1968, LTV Aerospace Corp., Dallas, Texas.

[3] J. L. Sims, "Table for Supersonic Flow Around Right Circular Cones at Zero Angle of Attack," SP-3004, 1964, NASA.

[4] B. J. Griffith and C. H. Lewis, "A Study of Laminar Heat Transfer to Spherically Blunted Cones and Hemisphere-Cylinders at Hypersonic Conditions," TDR-63-102, June 1963, Arnold Engineering Development Center, Tullahoma, Tenn.

[5] C. H. Lewis, "Pressure Distribution and Shock Shape Over Blunted Slender Cones at Mach Numbers from 16 to 19," TN-61-81, Aug. 1961, Arnold Engineering Development Center, Tullahoma, Tenn.

[6] M. E. Hillsamer and S. R. Mallard, "The Effects of Active Cooling on the Aerothermodynamic Characteristics of Slender Bodies of Revolution," TR-65-22, Feb. 1965, Arnold Engineering Development Center, Tullahoma, Tenn.

[7] C. J. Studerus, "Comparison of Theoretical and Experimental Induced Pressure Skin Friction Reduction, and Zero Lift Total Drag for a Pointed 7.5° Porous Cone in Presence of Turbulent Mass," Technical Information Ser. 65SD325, April 1965, General Electric, Missiles and Space Div., Philadelphia, Penn.

[8] A. J. Chapman, *Heat Transfer*, Macmillan, New York, 1960, Chap. 8.

[9] R. F. Probstein and D. Elliott, "The Transverse Curvature Effect in Compressible Axially Symmetric Laminar Boundary-Layer Flow," *Journal of the Aeronautical Sciences*, Vol. 23, No. 3, March 1956, pp. 208–224, 236.

[10] R. F. Probstein, "Interacting Hypersonic Laminar Boundary Layer Flow Over a Cone," TR AF 2798/1, March 1955, Aerospace Research Labs., Wright-Patterson Air Force Base, Dayton, Ohio.

[11] J. C. Hester and D. M. Martin, "Results of Heat Transfer Tests on Sharp and Spherically Blunted 4° Half Angle Conical Models in a Plasma Jet and In a Hypervelocity Wind Tunnel," Rept. 00.725, Dec. 1965, LTV Aerospac Corp., Dallas, Texas.

[12] T. A. Libby and R. J. Cresci, "The Downstream Influence of Mass Transfer at the Nose of Slender Cones," WADD-TR-60-892, Jan. 1962, Wright-Patterson Air Force Base, Dayton, Ohio.

[13] M. J. Brunner, "Active Cooling Heat Protection," AIAA Paper 68-1154, Williamsburg, Va., Dec. 1968.

[14] L. W. Carlson and E. Talmor, "Gaseous Film Cooling at Various Degrees of Hot-Gas Acceleration and Turbulence Levels," *International Journal of Heat and Mass Transfer*, Vol. 11, No. 11, Nov. 1968.

[15] M. W. Rubesin, "An Analytical Estimate of the Effect of Transpiration Cooling on Heat Transfer and Skin Friction Characteristics of a Compressible Turbulent Boundary Layer," TN 3341, Feb. 1965, NACA.

[16] M. W. Rubesin and C. C. Pappas, "An Analysis of the Turbulent Boundary Layer Characteristics of a Flat Plate with Distributed Light Gas Injection," TN 4149, Feb. 1958, NACA.

[17] J. B. Kelley et al., "Transpiration Cooling, Its Theory and Application," Rept. TM-66-5, June 1966, Jet Propulsion Center, Purdue Univ., Lafayette, Ind.

[18] H. A. Simon et al., "Transpiration Cooling Correlation for Air and Non-Air Free Streams," AIAA Paper 68-758, Los Angeles, June 1968.

[19] B. M. Leadon et al., "The Effects of Active Cooling on the Aerodynamic and Aerothermodynamic Characteristics of Slender Bodies of Revolution," AFFDL-TR-64-187, Dec. 1964, Wright-Patterson Air Force Base, Dayton, Ohio.

[20] B. J. Griffith and H. R. Little, "Mass Injection Studies on Slender Cones and a Flat Plate with Trailing-Edge Ramp at Mach Numbers from 9 to 21," TR-67-109, Aug. 1964, Arnold Engineering Development Center, Arnold Air Force Base, Tullahoma, Tenn.

[21] C. J. Scott, G. E. Anderson, and D. R. Elgin, "Laminar, Transitional and Turbulent Mass Transfer Cooling Experiments from Mach Numbers 3 to 5," Research Rept. 162, Aug. 1959, Univ. of Minnesota, Minneapolis, Minn.

[22] J. E. Danberg et al., "Heat and Mass Transfer in a Hypersonic Turbulent Boundary Layer," *Proceedings of the 1965 Heat Transfer and Fluid Mechanics Institute*, edited by A. F. Charwat, Stanford Univ. Press, Stanford, Calif., 1965.

[23] J. D. Whitfield and B. J. Griffith, "Viscous Effects on Zero-Lift Drag of Slender Blunt Cones," TDR-63-35, March 1963, Arnold Engineering Development Center, Arnold Air Force Base, Tullahoma, Tenn.

[24] J. D. Whitfield and W. Wolny, "Hypersonic Static Stability of Blunt Slender Cones," TDR-62-166, Aug. 1962, Arnold Engineering Development Center, Arnold Air Force Base, Tullahoma, Tenn.

[25] D. J. Eckstrom, "The Influence of Mass and Momentum Transfer on the Static Stability and Drag of a Slender Cone—An Experimental Correlation," IMSC/DO51269, July 1968, Lockheed Missiles and Space Co., Sunnyvale, Calif.

[26] G. T. Chrusciel and S. S. Chang, "Effects of Ablation and Hypersonic Aerodynamic Stability Characteristics," AIAA Paper 66-410, Los Angeles, June 1966.